*Human Molecular Genetics, 2014, Vol. 23, No. 10* **2593–2603**
*doi:10.1093/hmg/ddt655*
*Advance Access published on December 23, 2013*

# Human-specific microRNA regulation of FOXO1: implications for microRNA recognition element evolution

**Hayley S. McLoughlin[2], Ji Wan[3], Ryan M. Spengler[1], Yi Xing[4] and Beverly L. Davidson[1,2,3,*]**

[1]Department of Internal Medicine, Neurology, and Physiology and Biophysics, [2]Department of Neuroscience and University of California, Los Angeles, Los Angeles, USA [3]Department of Genetics, Interdisciplinary Graduate Program, University of Iowa, Iowa City, IA 52240, USA and [4]Department of Microbiology, Immunology, and Molecular Genetics, University of California, Los Angeles, Los Angeles, CA 90095, USA

Received September 16, 2013; Revised November 25, 2013; Accepted December 20, 2013

**MicroRNAs (miRNAs) have been established as important negative post-transcriptional regulators for gene expression. Within the past decade, miRNAs targeting transcription factors (TFs) has emerged as an important mechanism for gene expression regulation. Here, we tested the hypothesis that in TF 3′UTRs, human-specific single nucleotide change(s) that create novel miRNA recognition elements (MREs) contribute to species-specific differences in TF expression. From several potential human-specific TF MREs, one candidate, a member of the Forkhead Box O (FOXO) subclass in the Forkhead family known as Forkhead Box O1 (FOXO1; FKHR; NM_002015) was tested further. Human FOXO1 contains two sites predicted to confer miR-183-mediated post-transcriptional regulation: one specific to humans and the other conserved. Utilizing dual luciferase expression reporters, we show that only the human FOXO1 3′UTR contains a functional miR-183 site, not found in chimpanzee or mouse 3′untranslated regions (UTRs). Site-directed mutagenesis supports functionality of the human-specific miR-183 site, but not the conserved miR-183 site. Via overexpression and target site protection assays, we show that human FOXO1 is regulated by miR-183, but mouse FOXO1 is not. Finally, FOXO1-regulated cellular phenotypes, including cell invasion and proliferation, are impacted by miR-183 targeting only in human cells. These results provide strong evidence for human-specific gain of TF MREs, a process that may underlie evolutionary differences between phylogenic groups.**

## INTRODUCTION

MicroRNAs (miRNAs) are predicted to regulate between 30 and 66% of all protein-coding genes, ranking them among the largest classes of gene regulators (1,2). These ∼21–23 nucleotide non-coding RNAs function by post-transcriptionally silencing gene expression through imperfect base pairing of target messenger RNAs (mRNAs) to induce translational repression, deadenylation or degradation. Many miRNA gene families are highly conserved with implications in the regulation of many biological processes, including cell development, differentiation, metabolism, the cell cycle and ageing (3–5). The canonical miRNA recognition element (MRE) on a target mRNA consists of a perfect or near-perfect reverse complement of miRNA nucleotide positions 2 through 8 from the 5′ end (known as the seed region), together with partial complementarity throughout the rest of the miRNA and target transcript sequences. Prediction algorithms query mRNAs for reverse complement miRNA seed sequences to identify predicted MREs (6).

Insights into the evolution of miRNAs have emerged from bioinformatic analyses in whole animal studies, and suggest that selective pressure can impart their loss or conservation (7–9). Data support that *de novo* creation of miRNAs (*trans*-evolution) throughout speciation occurs, as evidenced through computational biology and reporter assay validation (10,11). Less is known, however, regarding species-specific evolution and the functional consequences of a single MRE through *cis*-evolution. Moreover, no investigation to date has directly assessed the human *cis*-evolutionary implications of the relationship between a miRNA and a target mRNA that encodes a transcription factor (TF), which can have broad implications via indirect regulation of TF target genes (12–16).

*To whom correspondence should be addressed: Department of Internal Medicine, University of Iowa, 200 Eckstein Medical Research Building, Iowa City, IA 52240, USA. Tel: +1 319 3535573; Fax: +1 319 3535572; Email: beverly-davidson@uiowa.edu

TFs can enhance or repress transcription of genes containing the corresponding TF consensus binding sequence. TF-regulated genes function as central hubs in well-established gene regulatory networks, for example, those that control the cell-cycle state or cell migration (17–21). Within the past decade miRNA–TF interactions have emerged as important mechanisms for gene expression regulation, acting either as buffers for gene expression or as quick repressive switches in a central hub (22–26). Interestingly, tissue- and species-specific miRNAs have a higher propensity to target TFs than expected (27). Together with work indicating that in humans, TF expression diverges more in the brain than in other tissues (28), we hypothesized that human-specific single nucleotide change(s) in a MRE of a TF 3′UTRs would contribute to species-specific differences in TF expression and subsequent downstream TF-regulated functional processes.

Here, we identified using bioinformatic methods candidate TF:MRE pairs that may be unique to TF regulation in human cells versus other mammals, including primates. We used wet lab approaches to fully characterize the functional implications of one of these, FOXO1, and show that FOXO1 is regulated by miR-183 in human cells through the gain of a single nucleotide substitution, and that this regulation is important for FOXO1-dependent functions, including proliferation and migration (17–20).

## RESULTS

### Selection of candidate human-specific MRE

To detect human-specific MREs, we first predicted human MREs in the 3′UTRs of human TFs. Next, we identified single nucleotide changes in human MREs in the 3′UTRs of orthologous TFs in chimpanzee (*Pan troglodytes*), rhesus macaque (*Macaca mulatta*) and mouse (*Mus musculus*). This bioinformatic analysis resulted in 198 human-specific MREs in 100 TFs for 136 conserved miRs. We supported our output by comparing our predictions with the PITA (Probability of Interaction by Target Accessibility) algorithm, which computes a ΔΔG score by subtracting the MRE openness score ($\Delta G_{open}$) from the binding energy of miRNA-target duplex ($\Delta G_{duplex}$) (Supplementary Material, Table S1). MiRNA sequence target prediction is greater when $\Delta\Delta G = \Delta G_{duplex} - \Delta G_{open}$ scores are $< -10$ units. Additionally, we completed a gene ontology analysis over orthologous genes with human-specific MREs and found that biological processes related to neuron and brain function are highly enriched (Supplementary Material, Table S2).

We chose four candidate human-specific TF MREs from the bioinformatic analysis for further validation. As the first round of validation for human-specific TF MREs, we cloned the human TF 3′UTRs into psiCHECK-2$^{TM}$ dual luciferase plasmid, downstream of *Renilla* luciferase to test for miRNA regulation using pre-miRNAs at increasing doses. We found that the human-specific predicted miR-145* site on RBPJ (recombining binding protein suppressor of hairless) and the miR-183 site on FOXO1 (Forkhead Box O1) showed significant decreases in luciferase expression relative to control pre-miRs (Fig. 1A and Fig. 2C). No evidence of luciferase expression regulation was found when co-transfecting pre-miR-7 or pre-miR-7* with psiCHECK$^{TM}$-2-NFYA (nuclear TF Y alpha) or psiCHECK$^{TM}$-2 MEF2A (myocyte enhancer factor-2a) plasmids, respectively (Fig. 1B and C).

### Human FOXO1 contains predicted miR-183 regulatory sites

Of the candidate TFs predicted to be regulated by human-specific MREs, FOXO1 was particularly interesting because its 3′UTR harbors both conserved and human-specific miR-183 sites (Fig. 2A). To determine the impact of two miR-183 MREs on the human FOXO1 mRNA relative to those from other species, we also amplified genomic DNA from chimpanzee and mouse FOXO1 3′UTRs and cloned them into psiCHECK$^{TM}$-2 dual luciferase plasmids downstream of *Renilla* luciferase. A positive control for miRNA regulation included a perfect target (PT) control cloned into the 3′UTR of *Renilla* luciferase. When the PT control plasmid was transfected into cells with pre-miR-183, there was significant silencing (Supplementary Material, Fig. S2). To test for miRNA regulation of the independent MREs, each 3′UTR reporter was co-transfected with increasing doses of synthetic pre-miR-183. We also tested the effects of both a scrambled control pre-miR-NEG and an additional irrelevant pre-miR-146b control, which

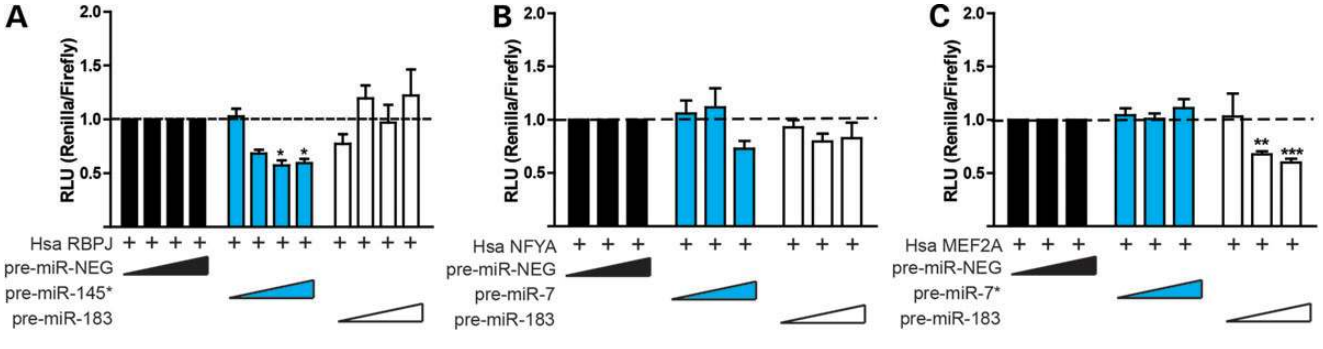


**Figure 1.** Human gain of target candidate validation of MRE in 3′UTR. Dual luciferase plasmids (psiCHECK$^{TM}$-2) containing the human 3′UTR of either RBPJ, NFYA or MEF2A were co-transfected with increasing doses of either pre-miR-NEG control (black), relevant pre-miR (blue) or irrelevant pre-miR control (white) into HEK293 cells. (**A**) Increasing expression of pre-miR-145* in cells transfected with psiCHECK$^{TM}$-2-RPBJ 3-UTR plasmid leads to a dose dependent decrease of RLU expression relative to controls pre-miRs. (**B** and **C**) No significant change in RLU expression was found when co-transfecting pre-miR-7 or pre-miR-7* with psiCHECK$^{TM}$-2-NFYA or psiCHECK$^{TM}$-2 MEF2A plasmids, respectively. (C) Interestingly, expression of pre-miR-183 in cells transfected with psiCHECK$^{TM}$-2-MEF2A 3-UTR plasmid led to a dose-dependent decrease of RLU expression relative to controls pre-miRs. Prediction databases validated this result as a conserved miR-183 target site in the MEF2A 3′UTR. All luciferase experiments were performed in triplicate for each pre-miR dose (0–30 nM). Each experiment was repeated in triplicate for each dose with at least three biological replicates. Bars represent mean ± SEM, $^{*}P < 0.05$, $^{**}P < 0.01$ and $^{***}P < 0.001$.

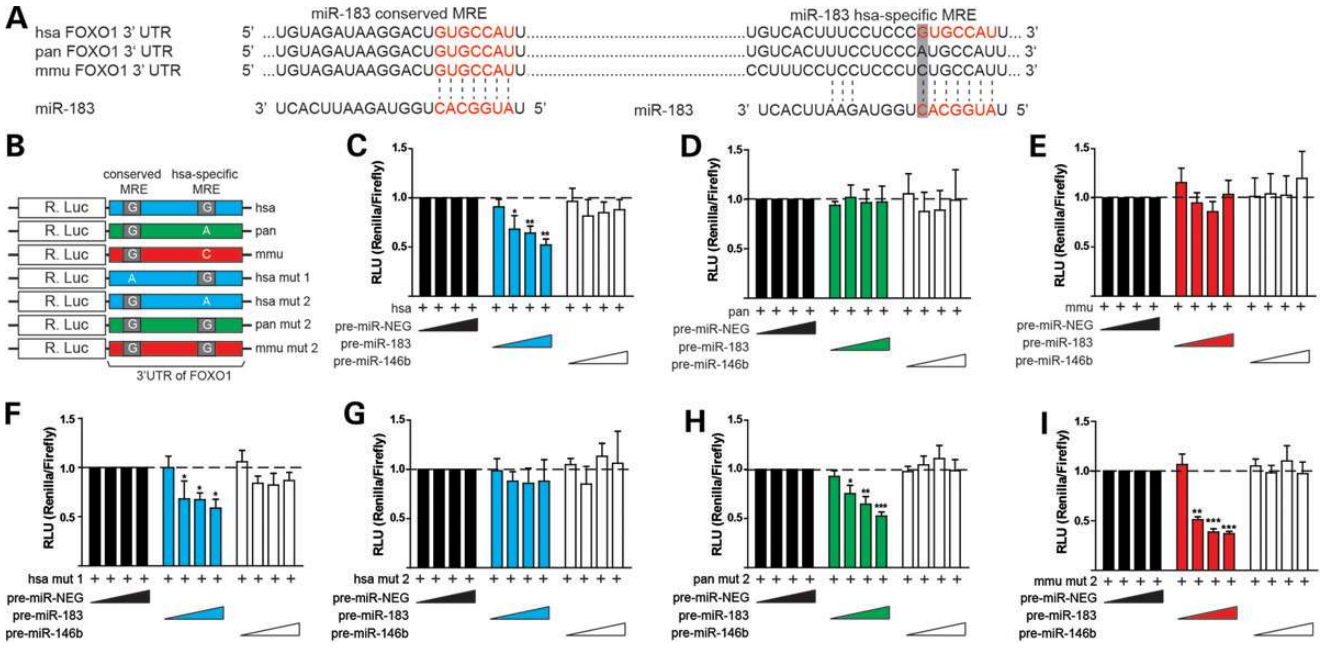


**Figure 2.** Regulation of hsa FOXO1 3′UTR by miR-183 MRE. (**A**) The schematic of FOXO1 with both the conserved and human-specific miR-183 prediction MREs in human (hsa), chimpanzee (pan) and mouse (mmu) 3′UTRs. (**B**) The schematic of FOXO1 3′UTR psiCHECK$^{TM}$-2 plasmids. PsiCHECK$^{TM}$-2 plasmids containing the 3′UTR of FOXO1 cloned from (**C**) hsa, (**D**) pan and (**E**) mmu were co-transfected with either pre-miR-NEG control, pre-miR-183 or irrelevant pre-miR-146b control into HEK293 cells. Single nucleotide changes in the psiCHECK$^{TM}$-2 3′UTR constructs included: (**F**) a nucleotide change at the conserved site of the hsa 3′UTR from G → A; (**G**) a nucleotide change at the hsa-specific miR-183 predict site in the hsa 3′UTR from G → A; (**H** and **I**) a mutation in pan and mmu 3′UTR from A → G or C → G, respectively. All luciferase experiments were performed in triplicate for each pre-miR dose (0–30 nM) with at least three biological replicates. Bars represent mean ± SEM, $^{*}P < 0.05$, $^{**}P < 0.01$ and $^{***}P < 0.001$.

is not predicted to target the FOXO1 3′UTR in any species. Co-transfection of pre-miR-183 and FOXO1 3′UTR reporter plasmids resulted in a dose-dependent reduction of luciferase constructs harboring the human FOXO1–3′UTR (Fig. 2B and C), but no change in chimpanzee (Fig. 2B and D) or mouse (Fig. 2B and E) FOXO1-3′UTR reporter constructs relative to negative controls. These data indicate that the conserved miR-183 MRE is not functional. Interestingly, the conserved human miR-183 site has a PITA-derived ΔΔG score of −1.86 and the human-specific miR-183 site a ΔΔG score of −10.35. Combined, these data suggest that the human-specific miR-183 site is more available for miRNA regulation than the conserved site (29).

To confirm that the single nucleotide difference in human FOXO1 3′UTR is the sole contributor to the functional human-specific miR-183 site, we completed site-directed mutagenesis to generate single nucleotide seed sequence changes, which either ablated the potential miR-183 MRE in the human-specific MRE or created a predicted miR-183 MRE in the chimpanzee and mouse 3′UTRs. We repeated the relative luciferase assay with these constructs and observed a dose-dependent reduction in the relative luciferase unit (RLU) expression in the chimpanzee (Fig. 2B and H) and mouse (Fig. 2B and I) FOXO1-3′UTR mutant constructs, which now match the human miR-183 MRE. Conversely, when the human-specific miR-183 site was mutated to match the analogous chimpanzee 3′UTR, miR-183 repression was lost (Fig. 2B and G). These results show that the single nucleotide change in human FOXO1 3-UTR is necessary and sufficient to induce miR-183 targeting in the context of the psiCHECK$^{TM}$-2 dual luciferase system. Interestingly, ablation of the conserved human miR-183 site via site-directed mutagenesis had no impact on luciferase expression relative to the normal FOXO1 human 3′UTR (Fig. 2B and F), indicating that the conserved miR-183 site in the human FOXO1 3′UTR is not functional.

### miR-183 targets endogenous FOXO1 at the human-specific MRE

Further evidence for human-specific regulation of FOXO1 expression by miR-183 was tested with the endogenous FOXO1 transcript as a target in human and mouse cell lines. While FOXO1 transcripts are ubiquitously expressed throughout the central nervous system, miR-183 is preferentially expressed in the cerebellum and striatum. Thus, we chose the human ONS-76 medulloblastoma cell line, which arises from granular cells, and the mouse C17-2 cerebellar stem cell line, also derived from granule cells (30). Both lines have robust FOXO1 and miR-183 expression (31). We first added exogenous pre-miR-183 and quantified FOXO1 mRNA levels by reverse transcription-quantitative polymerase chain reaction (RT-qPCR). Pre-miR-NEG and pre-miR-146b were used as negative controls. Results showed a dose-dependent decrease in FOXO1 transcripts in human ONS-76 cells transfected with pre-miR-183 (Fig. 3A), but no significant changes in FOXO1 levels in similarly treated mouse C17-2 cells (Fig. 3B). Western blot for FOXO1 protein levels following miR-183 transfection was consistent with this; there was decreased FOXO1 protein levels in miR-183 transfected ONS-76 cells (Fig. 3C),

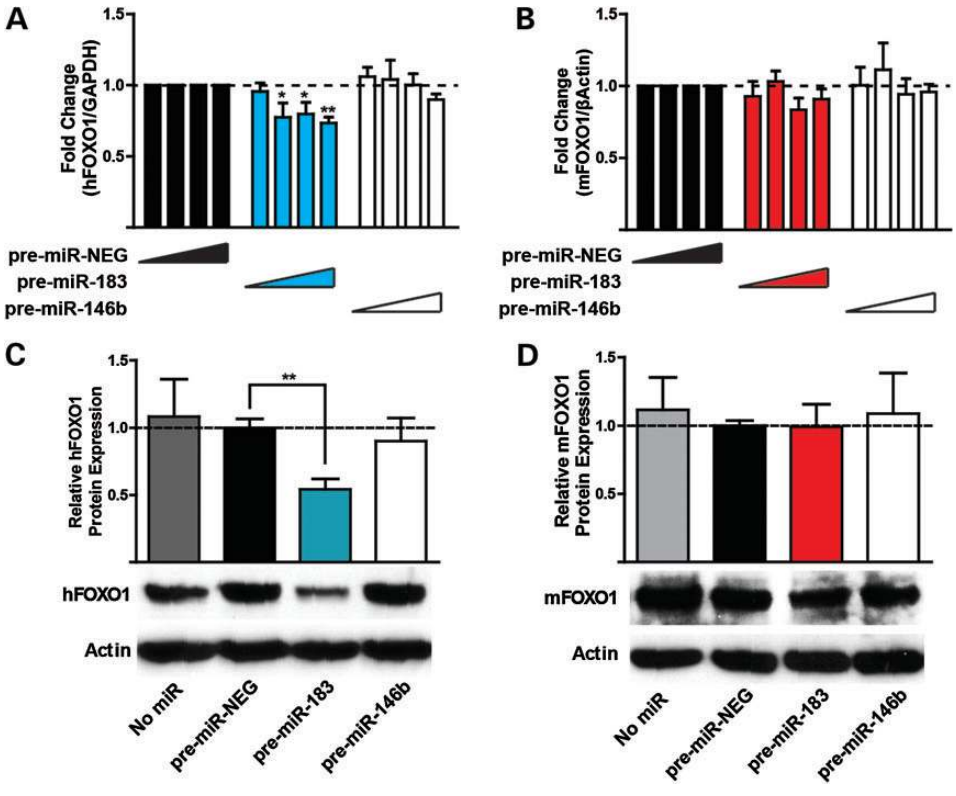


**Figure 3.** Pre-miR-183 modulates FOXO1 expression levels in hsa ONS-76 cells but not mmu C17–2 cells. Hsa ONS-76 and mmu C17-2 cells were transfected with increasing doses of either pre-miR-NEG control, pre-miR-183 or irrelevant pre-miR-146b control. Transfection of pre-miR-183 in hsa ONS-76 cells showed significant dose-dependent decreases in hsa FOXO1 (hFOXO1) (**A**) mRNA expression and (**C**) protein expression relative to control treatments. (**B**) Transfection of pre-miRs in mmu C17-2 cells results in no change to endogenous levels of mouse FOXO1 (mFOXO1) (B) mRNA or (**D**) protein. All mRNA experiments were performed in triplicate for each pre-miR dose (0–30 nM). Protein assessed after 30 nM pre-miR transfection. Each experiment was repeated in triplicate for each dose. Bars represent mean ± SEM, $^{*}P < 0.05$ and $^{**}P < 0.01$.

and no changes in C17-2 cells (Fig. 3D). These results confirm that in human ONS-76 cells, but not mouse cells, miR-183 can post-transcriptionally repress FOXO1 transcripts, causing significantly reduced human FOXO1 protein levels.

We next tested if endogenous miR-183 regulates endogenous FOXO1 transcripts. For this, we designed oligonucleotides to act as target site protectors (TSPs) to the miR-183 MREs. This provides a mechanism to test directly the functional activity of a given MRE on the transcript in question, without sponging away the miRNA from other potential targets. TSPs blocking the human-specific MRE (TSP2-183) or sequences that would recognize the corresponding mouse 3′UTR region of FOXO1 (does not contain a miR-183 MRE) were transfected into ONS-76 or C17-2 cells, respectively, and FOXO1 levels quantified by RT-qPCR and western blot. A scrambled negative control TSP (TSP-NEG) and TSP against the conserved miR-183 site (TSP1-183) were also tested. While there were no changes in transcript levels with any of the TSPs (Supplementary Material, Fig. S3A and B), we found that TSP2-183 significantly increased human FOXO1 protein levels relative to control-treated cells or TSP1-183-treated cells (Fig. 4A). This change in FOXO1 protein levels was not found in mouse C17-2 cells transfected with either TSP1-183 or TSP2-183 (Fig. 4B). These results confirm translational repression of FOXO1 protein at the human-specific miR-183 MRE in human cells.

### Functional implications of human FOXO1 regulation by miR-183: cellular invasion

FOXO1 plays a known role in transcriptionally regulating cell movement (32). In human medulloblastoma cell lines, altering miR-183 levels impacts metastasis and invasion (31). We next confirmed FOXO1's ability to affect cell invasion by transfecting siRNAs against FOXO1 in human ONS-76 and mouse C17-2 cells (Supplementary Material, Fig. S4) and assessed invasion using a Matrigel$^{TM}$ invasion assay. In both ONS-76 and C17-2 cells, there was increased invasion relative to control treatment (Supplementary Material, Fig. S5). To test whether miR-183 regulation of FOXO1 is responsible for this effect, we performed Matrigel$^{TM}$ invasion assays in cell lines after transfecting with pre-miRs. Overexpression of pre-miR-183 increased the number of invading cells after 24 h in human ONS-76 cells (Fig. 5A and B) relative to control pre-miRs, but did not affect cell invasion in mouse C17-2 cells (Fig. 5A and C). To determine whether increased migration after miR-183 transfection occurs through the human-specific MRE, we transfected ONS-76 or C17-2 cells with TSP2-183 or TSP-NEG. We found decreased invasion relative to TSP-NEG transfected cells in human ONS-76 cell lines (Fig. 6A and B), with no significant change in invasion in similarly treated mouse C17-2 cells (Fig. 6A and C).

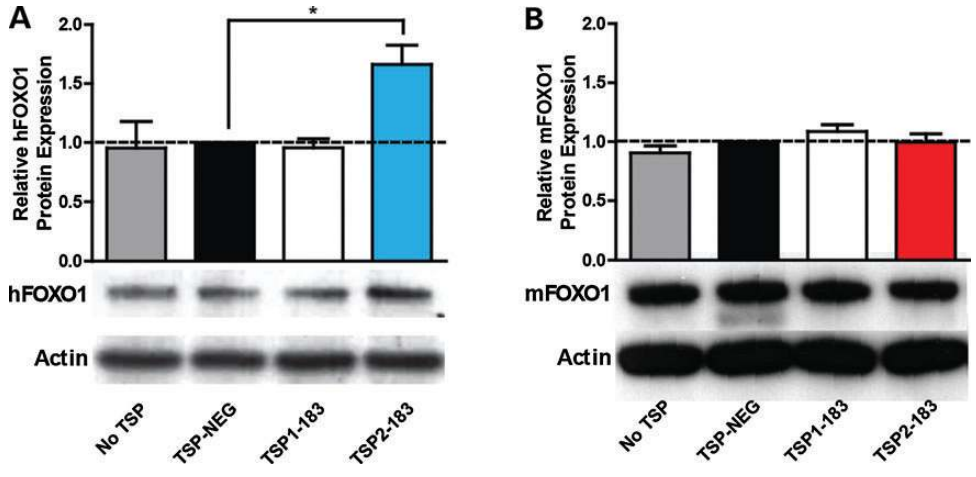


**Figure 4.** TSP of FOXO1 3′UTR regulates expression levels at the human-specific MRE in hsa ONS-76 cells. Hsa ONS-76 and mmu C17-2 cells were transfected with either TSP-NEG control, conserved TSP1-183 or human-specific TSP2-183. Transfection of TSPs in (**A**) hsa ONS-76 and (**B**) mmu C17-2 cells, showed significant changes in FOXO1 protein expression in TSP2-183 transfected hsa ONS-76 cells, but not mmu C17-2 cells. All experiments were performed in triplicate for each TSP (30 nM). Bars represent mean ± SEM, $^{*}P < 0.05$.

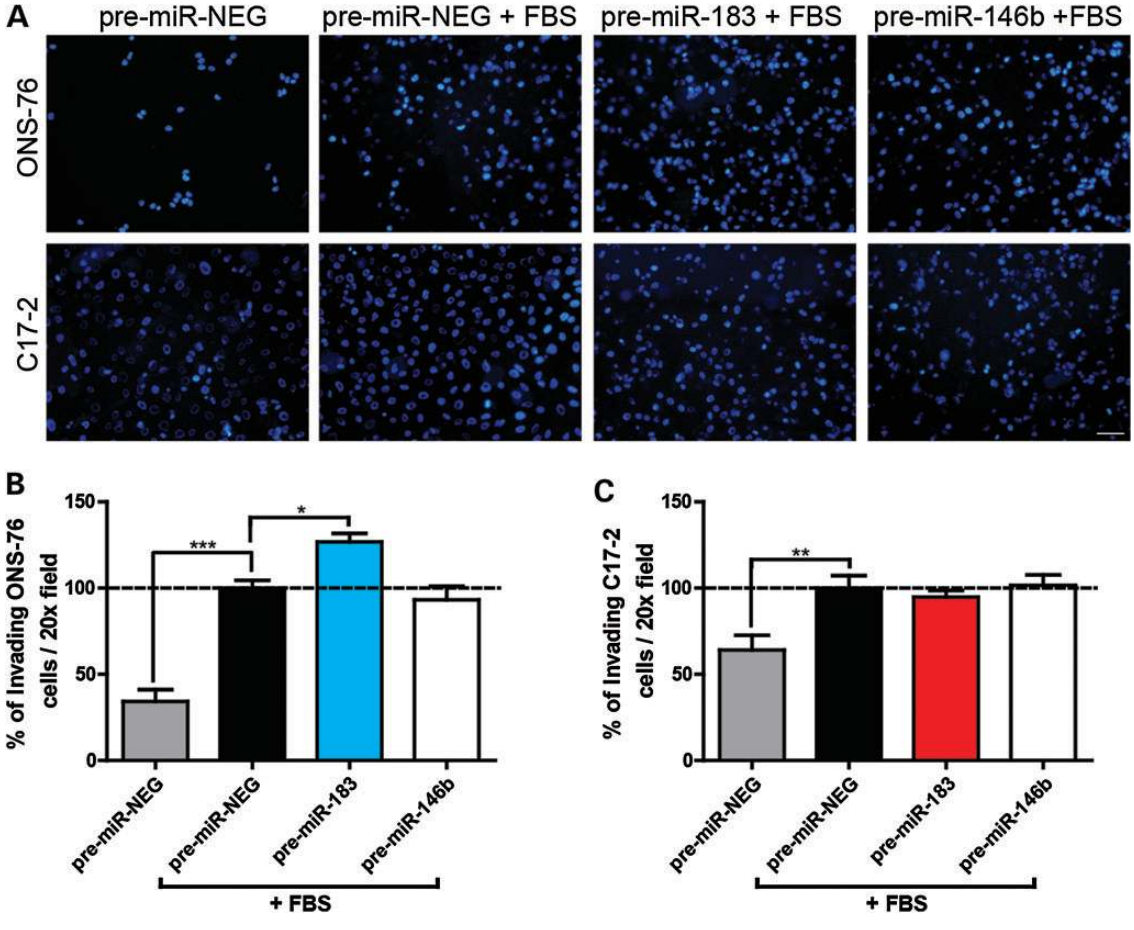


**Figure 5.** Pre-miR-183 induces cell invasion in hsa ONS-76 cells but not mmu C17-2 cells. Hsa ONS-76 and mmu C17-2 cells were transfected with 30 nM of either pre-miR-NEG control, pre-miR-183 or irrelevant pre-miR-146b control and plated into Matrigel™ transwells. (**A**) Representative images from a Matrigel™ transwell invasion show significant increase in cell invasion upon overexpression of pre-miR-183 in ONS-76 cells, but not in C17-2 cells. (**B**) Hsa ONS-76 and (**C**) mmu C17-2 migrated cells were quantified from 20× fields and normalized to the average number of pre-miR-NEG cells with FBS chemo-attractant in at least three independent experiments. Bars represent mean ± SEM, $^{*}P < 0.05$, $^{**}P < 0.01$ and $^{***}P < 0.001$.

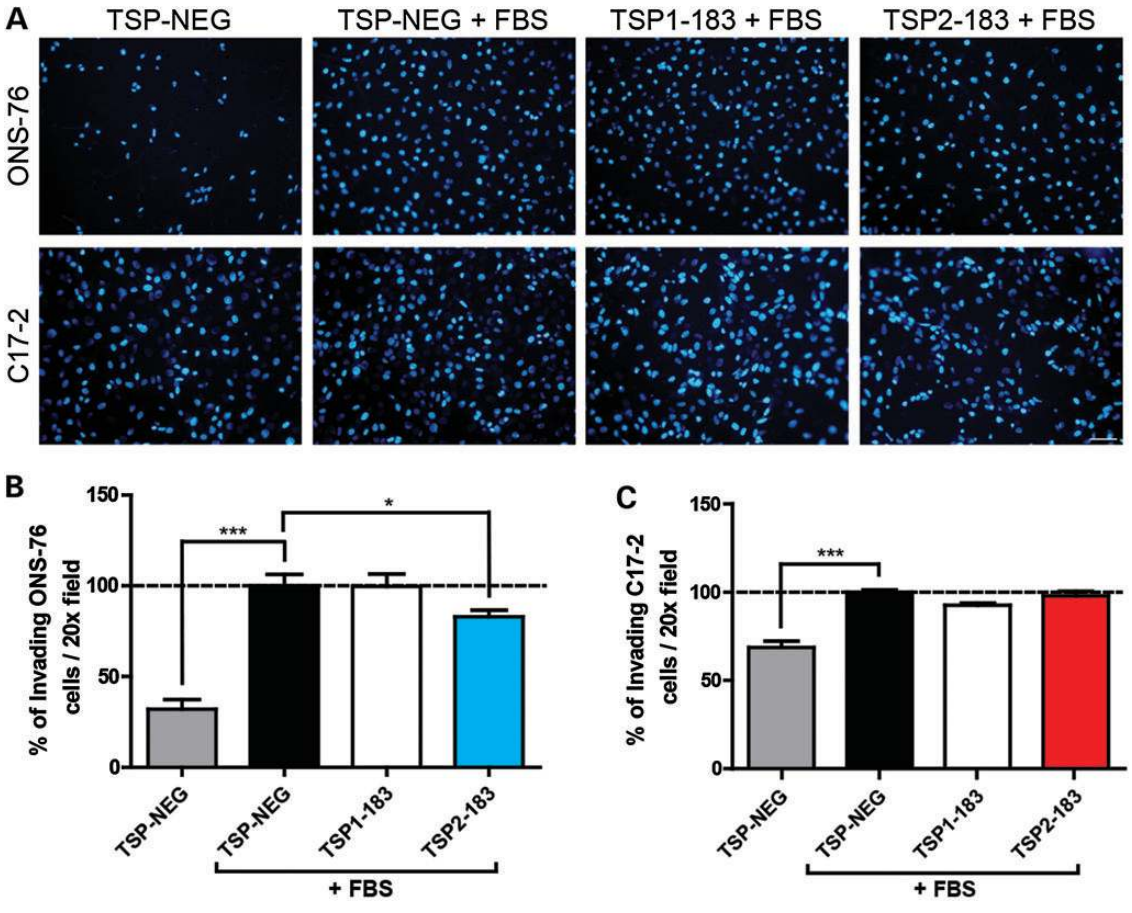


**Figure 6.** TSP of human-specific miR-183 MRE impedes cell invasion in hsa ONS-76 cells but not mmu C17-2 cells. Hsa ONS-76 and mmu C17-2 cells were transfected with 30 nM of either TSP-NEG control, conserved TSP1-183 or human-specific TSP2-183 and plated into Matrigel$^{TM}$ transwells. (**A**) Representative images from a transwell Matrigel$^{TM}$ invasion show significant decrease in cell invasion upon target-site protection with TSP2-183 in ONS-76 cells, but not in C17-2 cells. (**B**) Hsa ONS-76 and (**C**) mmu C17-2 migrated cells were quantified from 20× fields and normalized to the average number of TSP-NEG cells with FBS chemo-attractant in at least three independent experiments. Bars represent mean ± SEM, $^{*}P < 0.05$ and $^{***}P < 0.001$.

### Functional implications of human FOXO1 regulation by miR-183: cellular proliferation

FOXO1 is also implicated in transcriptional regulation of cell-cycle progression (33–35). We first validated this finding in our cell models using siRNAs against FOXO1. Using flow cytometry to determine 5-bromo-2′-deoxyuridine/propidium iodide (BrdU/PI) DNA content, we found that decreased FOXO1 expression caused corresponding increases in cells entering S-phase relative to control-treated cells (Supplementary Material, Fig. S6). We next tested whether FOXO1-mediated changes were recapitulated after overexpression of pre-miR-183 in human ONS-76 but not mouse C17-2 cells. Interestingly, quantification of BrdU/PI DNA content showed a decrease in the total number of cells entering S-phase after pre-miR-183 transfection in both human ONS-76 cells (Supplementary Material, Fig. S7A and B) and mouse C17-2 cells (Supplementary Material, Fig. S7A and C). This suggests that pre-miR-183 regulates cell proliferation in each of the tested cell lines. To test the relevance of the human-specific miR-183 MRE in proliferation, we transfected TSP2-183 and the analogous mouse FOXO1 3′UTR-specific TSP into ONS-76 cells and C17-2 cells, respectively. Quantification showed an increase in total number of cells entering S-phase when the human-specific miR-183 MRE is protected relative to a TSP-NEG in ONS-76 cells (Fig. 7A and B). No effect on cell cycle was found in mouse C17-2 cells transfected with sequences analogous to TSP2-183 (Fig. 7A and C). These results indicate that the human-specific miR-183 site and other miR-183 gene targets contribute to a cellular proliferation phenotype.

## DISCUSSION

One of the central sources of phenotypic evolution is changes in regulation of gene expression via mechanisms that act directly on the genome, such as TFs, or through post-transcriptional mechanisms, such as occurs with miRNAs (36). A potential source for positive selection by miRNA regulation is 3′UTR changes. Interestingly, work by Miura *et al.* (37) indicate that 3′UTRs in the mammalian brain are elongated by ∼5–6 Mb relative to all other mammalian tissues analyzed. Furthermore, *in silico* studies by Gardner *et al.* (38) implicate mutations causing functional loss of MREs during human evolution;

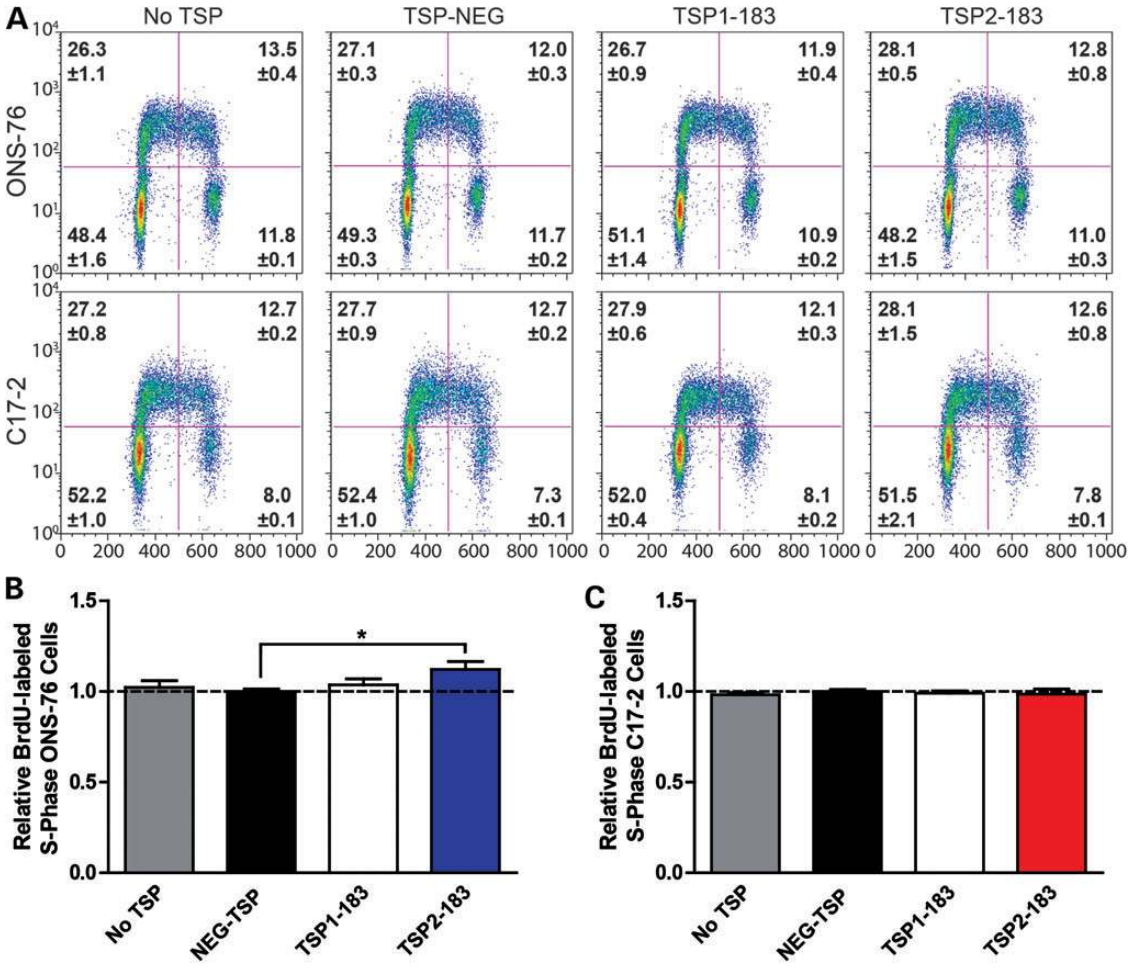


**Figure 7.** TSP of human-specific miR-183 MRE induces S-phase progression only in hsa ONS-76 cells. Hsa ONS-76 and mmu C17-2 cells were transfected with 30 nM of either TSP-NEG control, conserved TSP1-183 or human-specific TSP2-183. Prior to harvest, cells were pulsed with BrdU for 30 min under proliferating conditions and processed to determine BrdU incorporation (A488, y-axis) and DNA content (PI-A, x-axis). (**A**) Representative BrdU/PI dot plots are shown, and quadrant statistics for three replicate experiments are displayed on the dot plots (mean ± SEM of three experiments). (**B**) Hsa ONS-76 cells displayed significant increase in relative BrdU-positive S-phase cells upon overexpression of TSP2-183 relative to TSP-NEG, while (**C**) mmu C17-2 cells displayed no significant change. Bars represent mean ± SEM, $^{*}P < 0.05$.

however, no gain of function MRE analyses has been completed to date. Phenotypic differences within species may also be caused by changes in miRNA-mediated regulation of target transcripts. For example, the TYRP1 is regulated by miR-155, and changes in the MRE may underlie differences in skin pigmentation (39). Combining the two central sources of phenotypic evolution, miRNAs have been found to preferentially target genes with high regulatory complexity (e.g. TFs), and both TF and miRNA regulation have strong dependent effects on protein evolutionary rates (16,40,41). Together with our data showing gain of MRE target sites in TFs regulated by miRNAs, it is worth revisiting MREs in the context of large scale phenotypic evolution through novel targeting of TF 3′UTRs.

We first tested four candidate human-specific TF MRE sites and showed regulation by the predicted miRNA within two of the TF 3′UTRs, FOXO1 and RBPJ. Given the high false-positive rates of miRNA target prediction algorithms (42), we were encouraged that 50% of our tested *in silico* predictions are putative MREs. We went on to show that FOXO1 is regulated by miR-183 in human cells at a novel MRE site that arose from a single nucleotide substitution. Interestingly, the more conserved of the predicted sites was not functional. These data help clarify several conflicting reports regarding the role of miR-183 on the regulation of FOXO1. Stittrich *et al*. (20) reported earlier that increased miR-183 levels after IL-2 induction induced FOXO1, but concluded that the effect of miR-183 was indirect because only the contribution of the conserved miR-183-binding site on FOXO1was tested. In studies in endometrial cancer cells, elevated miR-183 correlated with reduced FOXO1 levels compared with control cells, and anti-miR experiments relieved this repression; however, direct testing of miR-183 MREs was not done (43). We find that the gain of the MRE is not present in chimpanzee or mice FOXO1 3′UTRs, indicating that this site arose after the split of humans and chimpanzees.

Our study shows that the human-specific MRE in FOXO1 impacts TF's expression and alters downstream phenotypes associated with FOXO1 levels, thus altering in a species-specific way these TF-regulated phenotypes. More specifically, we found that miR-183 elevation, or inhibition of its activity at the FOXO1 3′UTR MRE altered FOXO1 levels and impacted cell

invasion and proliferation in human cells. These results have relevance for human cancers, where FOXO1 is decreased and miR-183 levels are elevated (31,44–46). Interestingly, the FOXO1 transcript also contains predicted conserved and non-conserved MREs for the two other miRNAs in the miR-183/96/182 cluster, although neither miR-96 nor miR-182 were predicted in our analysis to be human-specific MREs. The predicted target sites of miR-182/96 in the FOXO1 3′UTR do not overlap with the target sites of miR-183, and thus do not contribute to competitive inhibition of miR-183 regulation. Additionally, PITA predictions of the non-conserved miR-182 and miR-96 sites indicate a low likelihood of targeting potential, similar to what was found for the non-functional, conserved miR-183 site. It would be interesting in subsequent work to evaluate the relationship of these miRNAs on FOXO1 regulation, especially in the context of cancer cell biology where this cluster is shown to be upregulated (47).

We used PITA to identify MREs of low ΔΔG score (ΔΔG $<10$ units), as described in the results section, with the idea that these may represent novel, human-specific TF MREs. In addition to the miR-183:FOXO1 interaction, miR-205 may target the human ras responsive element binding protein 1 (RREB1) 3′UTR. Interestingly, RREB1 is a human oncogene and miR-205 is a putative tumor suppressor (48–50). Moreover, the TF-specific protein 1 (Sp1) has two conserved miR-7 MREs and one human-specific miR-7 MRE that provide for additive regulation in human brain tissue, where both Sp1 and miR-7 are highly expressed (51). Individually, Sp1 and miR-7 dysregulation has been found in many cancers and neurodegenerative disorders, but their relationship has not been defined.

While we defined *in silico* predictions based on canonical seed sequence complementarity, non-canonical miRNA:mRNA target interactions have been shown to be functional (52,53). Also, recent work suggests that miRNAs can target coding, intronic and 5′UTR regions, although these predicted binding sites have low validation rates. Further experimental analyses of the TF:MRE sites presented here should consider MRE accessibility with relation to both mRNA secondary structure and protein-regulated site competition, as well as miRNA and mRNA co-expression in the tissue or cell of interest (27,36). Several methods to identify bona fide targets include HITS-CLIP (High-throughput sequencing of RNA isolated by crosslinking immunoprecipitation), PAR-CLIP (Photoactivatable-Ribonucleoside-Enhanced Crosslinking and Immunoprecipitation) and CLASH (crosslinking, ligation, and sequencing of hybrids) (54–56). Chi *et al.* (55) generated the first mouse brain transcriptome-wide Ago2 binding map, with many Ago2 footprints in 3′UTRs, coding regions and introns corresponding to known, highly enriched, brain mRNAs. A similar investigation in human brain samples will increase our understanding of how miRNA regulation on brain transcripts participates in evolutionary speciation.

## MATERIALS AND METHODS

### Bioinformatic analysis

We retrieved human mature miR sequences (miRBase release16) (57) and their orthologous sequences in chimpanzee (panTro2), rhesus macaque (rheMac2) and mouse (mm9) from the UCSC 46-way alignment of the human genome and 45 other vertebrate genomes (http://hgdownload.soe.ucsc.edu/goldenPath/hg19/multiz46way/) (58). The 347 mature miR families with conserved seed regions (second to eighth position of the mature miR) in all four species were retained for MRE prediction. We used TargetScan (59) to predict the MREs of conserved miRs in the Ensembl 3′UTRs (Ensembl release 63) of 245 human TFs, which were compiled from TRANSFAC® database (60) and filtered for (i) one-to-one orthologous genes in chimpanzee, rhesus macaque and mouse based on Ensembl annotation (61) and (ii) the availability of corresponding ChIP-Seq data in ENCODE project. Next, predicted human MREs were compared with their orthologous sequences in chimpanzee, rhesus macaque and mouse. If none of the orthologous sequences of a human MRE forms a canonical base pairing with the miR according to TargetScan, it is defined as a human-specific MRE. To focus only on fixed human-specific MREs, Human dbSNP 138 database was searched for SNPs at the mutation sites of human-specific MREs. The allele frequency data were retrieved from 1000 Genomes Human Genetic Variation Project (http://www.1000genomes.org/data). This analysis identified 198 human-specific MREs from 136 miRs on 100 TFs.

### PITA target-site predictions

Binding energies were calculated for each miRNA/target site pair identified as being a human-specific TF MREs using the standalone implementation of the PITA target prediction algorithm (http://genie.weizmann.ac.il/pubs/mir07/mir07_exe.html). Target sites overlapping the human-specific TF MREs were identified. Binding energies (ΔΔG) are reported as the average score for all miRNAs in the respective miRNA families.

### Cultures

Human embryonic kidney 293 cells (HEK293) and ONS-76 cells were cultured in Dulbecco's modified Eagle's medium (DMEM) (Gibco-BRL, Grand Island, NY, USA) supplemented with 10% fetal bovine serum and 1% Penicillin/Streptomycin. Mouse C17-2 cerebellar stem cells were cultured in DMEM supplemented with 10% fetal bovine serum, 5% equine serum, 1% Penicillin/Streptomycin and 1% L-glutamine. All cells were incubated at 37°C in a 5% $CO_2$ atmosphere.

### psiCHECK™-2 dual luciferase 3′UTR plasmids

The 3′UTRs of candidate TFs from human, chimp and mouse were amplified from genomic DNA of human HEK293, chimp fibroblast cell lines and mouse tail fibroblasts using Expand High Fidelity DNA polymerase (Roche Applied Science) and 3′UTR-specific primers (designed using the Primer3 software and purchased from Integrated DNA Technologies) (Supplementary Material). Cloned PCR products were ligated into Topo TA plasmid and maintained as stock. Validation of correct PCR product insertion into Topo TA plasmid was confirmed through restriction enzyme digestion and Sanger sequencing. Proper PCR amplicons were digested out of Topo TA plasmid and ligated into a psiCHECK™-2 dual luciferase plasmid downstream of Renilla luciferase.

### Perfect target luciferase controls

Artificial 3′UTR PT controls were created to control for pre-miR silencing efficiency. PTs were created by complexing 8 μM of sense and antisense oligonucleotides containing a site with perfect complementarity to the mature miRNA with random flanking sequence and restriction sites (Supplementary Material). PCR cycles were performed three times at 94°C for 3 min, oligo Tm°C for 2 min and 72°C for 15 min. Purified sequences were cloned downstream of Renilla luciferase.

### psiCHECK$^{TM}$ -2 dual luciferase assay

HEK293 cells were transfected on 24-well plates using Lipofectamine 2000 (Invitrogen, CA, USA) per manufacturer's instructions to facilitate co-transfection of 4 ng of psiCHECK$^{TM}$-2 3′UTR plasmids and 0–30 nM of artificial precursor miRNAs (pre-miRs): pre-miR of interest, irrelevant control pre-miR or a NEG-control pre-miR. Artificial pre-miRs were purchased from Life Technologies: pre-miR-NEG 2 (AM17111), pre-miR-183-5p (PM12830) and pre-miR-146b (PM10105). Transfection media was completely removed 24 h post-transfection and cells were washed in ice-cold PBS. RLUs were measured according to the manufacturer's instructions (Promega) using a moon light luminometer (Pharmingen). Dual luciferase assays are reported by normalizing Renilla luciferase values to firefly luciferase values and normalized relative to controls. All experiments are performed in triplicate for each dose with a total of three experiments ($n = 3$) for statistical analysis. Data represent an average of the triplicates for each condition.

### Site-directed mutagenesis

Using the psiCHECK-2 dual luciferase plasmids with candidate TF 3′UTRs, single nucleotide mutations were made in the predicted human-specific MREs using the Phusion Site-Directed Mutagenesis Kit according to the manufacturer's instructions (Finnzymes) (Supplementary Material). All constructs were sequenced across both junctions to confirm the correct 3′UTR target was inserted with the proper orientation and sequence.

### Overexpression *in vitro* studies

*In vitro* expression assays were completed in both human ONS-76 medulloblastoma cell line and mouse C17-2 cerebellar stem cell line. For all expression assay experiments, we used RNAimax as per the manufacturer's instructions for more efficient transfection of small RNAs. Overexpression assays consisted of cells transfected with 0–30 nM of artificial pre-miR as described in psiCHECK$^{TM}$-2 Dual Luciferase Assays.

### Target site protectors transfections

Target site protectors (TSPs) were designed as a variant on the ZEN$^{TM}$-AMO (Anti-miRNA Oligonucleotides) chemistry design from Integrated DNA Technologies, Coralville, IA, USA (Supplementary Material). Each TSP sequence contains 2-*O*-methyl RNA nucleotides and a ZEN non-nucleotide modifier between the first two and last two nucleotides of each sequence. TSP assays consisted of cells transfected with 30 nM of TSP. Experiments were performed using TSP against the conserved miR-183 (TSP1-183), the human-specific miR-183 site (TSP2-183) or a negative control TSP (TSP-NEG) at a final concentration of 30 nM.

### RNA isolation and RT-qPCR analysis

Total RNA was isolated from cells 24 h post-transfection using Trizol reagent according to manufacturer's protocol (Invitrogen). RT was performed on 1 μg of total RNA using the High Capacity cDNA Reverse Transcriptase kit according to the manufacturer's instructions (Invitrogen). The cDNA was diluted 1:15 in $ddH_20$. Taqman relative quantification PCR was performed on the diluted cDNA of total RNA following the manufacturer's protocol (Applied Biosystems, Foster City, CA, USA) and results normalized to total RNA. Analysis was performed using average adjusted relative quantification on the following probes from Applied Biosystems: FOXO1 (Hs01054576_m1, Mm00490672_m1), Human GAPDH (4326317E), Mouse β-Actin (4352341E), miR-183-5p (002269), RNU48 (1006) and Sno202 (1232).

### Western blot assay

Protein was harvested using RIPA buffer (Pierce) and 1 × protease inhibitor using standard techniques and quantified using $D_C$ Protein Assay (Bio-Rad). Protein extracts were separated on a 4–12% Bis-Tris Gel with MES (Invitrogen) and transferred to Immobilon 0.45 μm PVDF (polyvinylidene difluoride) transfer membranes (Millipore). Primary antibodies to FOXO1 (1:200; sc-11350; Santa Cruz Biotechnology, Inc.) and β-Actin (1:2,500; A5441; Sigma) were used. Blots were developed using ECL Plus Western Blotting Detection System (GE Healthcare) and quantified by VercaDoc 5000 MP (Bio-Rad Laboratories, Inc.)

### Invasion assay

Human ONS-76 and mouse C17-2 cell lines were cultured and transfected according to techniques described. Prior to transfection, cells were serum starved in 0.5% serum culture media. Following 24 h transfection, upper chambers of Mitragel$^{TM}$ Invasion Chambers (354480; BD Biosciences) with 8 μm pores were seeded with $1.0 \times 10^5$ transfected cells in 0.5% serum culture media and placed in 24-well dishes containing 10% serum culture media. Cells were allowed to migrate to underside of membrane for 24 h, then gently washed in cold PBS and fixed in 4% paraformaldehyde for 10 min. Non-invading cells were removed by gently wiping upper chamber with cotton-tipped swab. Invaded cells were incubated in Hoechst (1:5000; 33342; Sigma), washed and imaged by a Leica Leitz DMR fluorescent microscope at 20 × magnification. Cell counts were determined using the ImageJ software (Rasband, W.S., ImageJ, U.S. National Institute of Health, Bethesda, MD, USA, http://imagej.nih.gov/ij, 1997–2011). All cell counts were normalized to negative control + FBS (fetal bovine serum) condition. All experiments were performed in triplicate.

### PI flow cytometric analysis for DNA content

Human ONS-76 and mouse C17-2 cell lines were cultured and transfected according to technique describe above. BrdU/PI cell-cycle analysis (similar to Fineberg *et al*. (62). Thirty minutes prior to cell harvest, BrdU (20 μM, Sigma) was added to cell media for S-phase cell integration. At harvest, cells were dissociated with 0.25% trypsin, pelleted, washed in ice-cold PBS and resuspended in 0.4 ml of ice-cold PBS. While vortexing, 3.6 ml of ice-cold 95% EtOH was added to cells incubated at room temperature (RT) for 45 min. Cells were then washed in PBS-TB (PBS with 0.2% Tween and 0.1% bovine serum albumin) and re-suspended in 0.3 ml of 2 N HCL and incubated for 30 min in the dark at RT. To neutralize, 0.9 ml of 0.1 M sodium tetraborate was added to acidic cell solution. Pelleted cells were washed and incubated with PBS-TB diluted anti-BrdU (1:50, BD Biosciences #347580) overnight at 4°C on the rocker. Cells were washed 2× in PBS-TB and incubated with Alexa Fluor-488-conjugated goat anti-mouse IgG (Invitrogen) for 30 min at RT in the dark. Pelleted and washed cells were then re-suspension in 500 μl fresh PI/RNaseA solution (PBS with PI at 20 μg/ml, RNaseA at 200 μg/ml and 0.05% tween-20) and incubated in the dark for 30 min at RT. Cell samples were stored up to 1 day at 4°C before being collected on Becton Dickinson LSR II with UV at the University of Iowa Flow Cytometry Facility (http://www.healthcare.uiowa.edu/corefacilities/flowcytometry/). Fifteen thousand single-nuclei events were acquired and analyzed using the FlowJo software to determine cell-cycle proportions in quadrants. Upper left and upper right quadrants represent all S-phase BrdU-positive cells. The lower left indicates G1 phase cells and lower right indicates G2/M phase cells. All experiments were performed in triplicate.

### Statistics

Statistical significance was determined using either Student's unpaired *t*-test, one-way analysis of variance (ANOVA) followed by Dunnettt's *post hoc* analysis or two-way ANOVA followed by Bonferroni *post hoc* analysis (GraphPad Prism software, San Diego CA, USA).

## ACKNOWLEDGEMENTS

The authors acknowledge Seth Brown and members of the Xing and Davidson Labs.

*Conflict of Interest statement*. None declared.

## FUNDING

This work was supported by the Roy J. Carver Trust and the March of Dimes.

## REFERENCES

1. Lewis, B.P., Burge, C.B. and Bartel, D.P. (2005) Conserved seed pairing, often flanked by adenosines, indicates that thousands of human genes are microRNA targets. *Cell*, **120**, 15–20.
2. Friedman, R.C., Farh, K.K., Burge, C.B. and Bartel, D.P. (2009) Most mammalian mRNAs are conserved targets of microRNAs. *Genome Res.*, **19**, 92–105.
3. Roux, J., Gonzalez-Porta, M. and Robinson-Rechavi, M. (2012) Comparative analysis of human and mouse expression data illuminates tissue-specific evolutionary patterns of miRNAs. *Nucleic Acids Res.*, **40**, 5890–5900.
4. McLoughlin, H.S., Fineberg, S.K., Ghosh, L.L., Tecedor, L. and Davidson, B.L. (2012) Dicer is required for proliferation, viability, migration and differentiation in corticoneurogenesis. *Neuroscience*, **223**, 285–295.
5. Fineberg, S.K., Kosik, K.S. and Davidson, B.L. (2009) MicroRNAs potentiate neural development. *Neuron*, **64**, 303–309.
6. Griffiths-Jones, S., Moxon, S., Marshall, M., Khanna, A., Eddy, S.R. and Bateman, A. (2005) Rfam: annotating non-coding RNAs in complete genomes. *Nucleic Acids Res.*, **33**, D121–D124.
7. Heimberg, A.M., Sempere, L.F., Moy, V.N., Donoghue, P.C. and Peterson, K.J. (2008) MicroRNAs and the advent of vertebrate morphological complexity. *Proc. Natl. Acad. Sci. USA*, **105**, 2946–2950.
8. Peterson, K.J., Dietrich, M.R. and McPeek, M.A. (2009) MicroRNAs and metazoan macroevolution: insights into canalization, complexity, and the Cambrian explosion. *Bioessays*, **31**, 736–747.
9. Mohammed, J., Flynt, A.S., Siepel, A. and Lai, E.C. (2013) The impact of age, biogenesis, and genomic clustering on Drosophila microRNA evolution. *RNA*, **19**, 1295–1308.
10. Berezikov, E. (2011) Evolution of microRNA diversity and regulation in animals. *Nat. Rev. Genet.*, **12**, 846–860.
11. Berezikov, E., Thuemmler, F., van Laake, L.W., Kondova, I., Bontrop, R., Cuppen, E. and Plasterk, R.H. (2006) Diversity of microRNAs in human and chimpanzee brain. *Nat. Genet.*, **38**, 1375–1377.
12. Shalgi, R., Lieber, D., Oren, M. and Pilpel, Y. (2007) Global and local architecture of the mammalian microRNA-transcription factor regulatory network. *PLoS Comput Biol*, **3**, e131.
13. Cheng, C., Yan, K.K., Hwang, W., Qian, J., Bhardwaj, N., Rozowsky, J., Lu, Z.J., Niu, W., Alves, P., Kato, M. *et al.* (2011) Construction and analysis of an integrated regulatory network derived from high-throughput sequencing data. *PLoS Comput. Biol.*, **7**, e1002190.
14. Yu, X., Lin, J., Zack, D.J., Mendell, J.T. and Qian, J. (2008) Analysis of regulatory network topology reveals functionally distinct classes of microRNAs. *Nucleic Acids Res.*, **36**, 6494–6503.
15. Li, J., Hua, X., Haubrock, M., Wang, J. and Wingender, E. (2012) The architecture of the gene regulatory networks of different tissues. *Bioinformatics*, **28**, i509–i514.
16. Cui, Q., Yu, Z., Pan, Y., Purisima, E.O. and Wang, E. (2007) MicroRNAs preferentially target the genes with high transcriptional regulation complexity. *Biochem. Biophys. Res. Commun.*, **352**, 733–738.
17. Srivastava, V.K., Yasruel, Z. and Nalbantoglu, J. (2009) Impaired medulloblastoma cell survival following activation of the FOXO1 transcription factor. *Int. J. Oncol.*, **35**, 1045–1051.
18. Greer, E.L. and Brunet, A. (2008) FOXO transcription factors in ageing and cancer. *Acta Physiol. (Oxford)*, **192**, 19–28.
19. Xu, J., Li, R., Workeneh, B., Dong, Y., Wang, X. and Hu, Z. (2012) Transcription factor FoxO1, the dominant mediator of muscle wasting in chronic kidney disease, is inhibited by microRNA-486. *Kidney Int*, **82**, 401–11.
20. Stittrich, A.B., Haftmann, C., Sgouroudis, E., Kuhl, A.A., Hegazy, A.N., Panse, I., Riedel, R., Flossdorf, M., Dong, J., Fuhrmann, F. *et al.* (2010) The microRNA miR-182 is induced by IL-2 and promotes clonal expansion of activated helper T lymphocytes. *Nat. Immunol.*, **11**, 1057–1062.
21. Erwin, D.H. and Davidson, E.H. (2009) The evolution of hierarchical gene regulatory networks. *Nat. Rev. Genet.*, **10**, 141–148.
22. Zhao, C., Sun, G., Li, S. and Shi, Y. (2009) A feedback regulatory loop involving microRNA-9 and nuclear receptor TLX in neural stem cell fate determination. *Nat. Struct. Mol. Biol.*, **16**, 365–371.
23. Packer, A.N., Xing, Y., Harper, S.Q., Jones, L. and Davidson, B.L. (2008) The bifunctional microRNA miR-9/miR-9* regulates REST and CoREST and is downregulated in Huntington's disease. *J. Neurosci.*, **28**, 14341–14346.
24. Cheng, L.C., Pastrana, E., Tavazoie, M. and Doetsch, F. (2009) miR-124 regulates adult neurogenesis in the subventricular zone stem cell niche. *Nat. Neurosci.*, **12**, 399–408.
25. Shibata, M., Nakao, H., Kiyonari, H., Abe, T. and Aizawa, S. (2011) MicroRNA-9 regulates neurogenesis in mouse telencephalon by targeting multiple transcription factors. *J. Neurosci.*, **31**, 3407–3422.

26. Iwama, H. (2013) Coordinated networks of microRNAs and transcription factors with evolutionary perspectives. *Adv. Exp. Med. Biol.*, **774**, 169–187.
27. Dannemann, M., Prufer, K., Lizano, E., Nickel, B., Burbano, H.A. and Kelso, J. (2012) Transcription factors are targeted by differentially expressed miRNAs in primates. *Genome Biol. Evol.*, **4**, 552–564.
28. Nowick, K., Gernat, T., Almaas, E. and Stubbs, L. (2009) Differences in human and chimpanzee gene expression patterns define an evolving network of transcription factors in brain. *Proc. Natl. Acad. Sci. USA*, **106**, 22358–22363.
29. Kertesz, M., Iovino, N., Unnerstall, U., Gaul, U. and Segal, E. (2007) The role of site accessibility in microRNA target recognition. *Nat. Genet.*, **39**, 1278–1284.
30. Ryder, E.F., Snyder, E.Y. and Cepko, C.L. (1990) Establishment and characterization of multipotent neural cell lines using retrovirus vector-mediated oncogene transfer. *J. Neurobiol.*, **21**, 356–375.
31. Weeraratne, S.D., Amani, V., Teider, N., Pierre-Francois, J., Winter, D., Kye, M.J., Sengupta, S., Archer, T., Remke, M., Bai, A.H. *et al.* (2012) Pleiotropic effects of miR-183∼96∼182 converge to regulate cell survival, proliferation and migration in medulloblastoma. *Acta Neuropathol.*, **123**, 539–552.
32. Huynh, M.A., Ikeuchi, Y., Netherton, S., de la Torre-Ubieta, L., Kanadia, R., Stegmuller, J., Cepko, C., Bonni, S. and Bonni, A. (2011) An isoform-specific SnoN1-FOXO1 repressor complex controls neuronal morphogenesis and positioning in the mammalian brain. *Neuron*, **69**, 930–944.
33. Nakamura, N., Ramaswamy, S., Vazquez, F., Signoretti, S., Loda, M. and Sellers, W.R. (2000) Forkhead transcription factors are critical effectors of cell death and cell cycle arrest downstream of PTEN. *Mol. Cell Biol.*, **20**, 8969–8982.
34. Ramaswamy, S., Nakamura, N., Sansal, I., Bergeron, L. and Sellers, W.R. (2002) A novel mechanism of gene regulation and tumor suppression by the transcription factor FKHR. *Cancer Cell*, **2**, 81–91.
35. Schmidt, M., Fernandez de Mattos, S., van der Horst, A., Klompmaker, R., Kops, G.J., Lam, E.W., Burgering, B.M. and Medema, R.H. (2002) Cell cycle inhibition by FoxO forkhead transcription factors involves downregulation of cyclin D. *Mol. Cell Biol.*, **22**, 7842–7852.
36. Hobert, O. (2008) Gene regulation by transcription factors and microRNAs. *Science*, **319**, 1785–1786.
37. Miura, P., Shenker, S., Andreu-Agullo, C., Westholm, J.O. and Lai, E.C. (2013) Widespread and extensive lengthening of 3′ UTRs in the mammalian brain. *Genome Res.*, **23**, 812–825.
38. Gardner, P.P. and Vinther, J. (2008) Mutation of miRNA target sequences during human evolution. *Trends Genet.*, **24**, 262–265.
39. Li, J., Liu, Y., Xin, X., Kim, T.S., Cabeza, E.A., Ren, J., Nielsen, R., Wrana, J.L. and Zhang, Z. (2012) Evidence for positive selection on a number of MicroRNA regulatory interactions during recent human evolution. *PLoS Genet.*, **8**, e1002578.
40. Pelaez, N. and Carthew, R.W. (2012) Biological robustness and the role of microRNAs: a network perspective. *Curr. Top Dev. Biol.*, **99**, 237–255.
41. Chen, Y.C., Cheng, J.H., Tsai, Z.T., Tsai, H.K. and Chuang, T.J. (2013) The impact of trans-regulation on the evolutionary rates of metazoan proteins. *Nucleic Acids Res*, **41**, 6371–80.
42. Saito, T. and Saetrom, P. (2010) MicroRNAs—targeting and target prediction. *N. Biotechnol.*, **27**, 243–249.
43. Myatt, S.S., Wang, J., Monteiro, L.J., Christian, M., Ho, K.K., Fusi, L., Dina, R.E., Brosens, J.J., Ghaem-Maghami, S. and Lam, E.W. (2010) Definition of microRNAs that repress expression of the tumor suppressor gene FOXO1 in endometrial cancer. *Cancer Res.*, **70**, 367–377.
44. Jalvy-Delvaille, S., Maurel, M., Majo, V., Pierre, N., Chabas, S., Combe, C., Rosenbaum, J., Sagliocco, F. and Grosset, C.F. (2012) Molecular basis of differential target regulation by miR-96 and miR-182: the Glypican-3 as a model. *Nucleic Acids Res.*, **40**, 1356–1365.
45. Gokhale, A., Kunder, R., Goel, A., Sarin, R., Moiyadi, A., Shenoy, A., Mamidipally, C., Noronha, S., Kannan, S. and Shirsat, N.V. (2010) Distinctive microRNA signature of medulloblastomas associated with the WNT signaling pathway. *J. Cancer Res. Ther.*, **6**, 521–529.
46. Wang, G., Mao, W. and Zheng, S. (2008) MicroRNA-183 regulates Ezrin expression in lung cancer cells. *FEBS Lett.*, **582**, 3663–3668.
47. Guttilla, I.K. and White, B.A. (2009) Coordinate regulation of FOXO1 by miR-27a, miR-96, and miR-182 in breast cancer cells. *J. Biol. Chem.*, **284**, 23204–23216.
48. Wu, H., Zhu, S. and Mo, Y.Y. (2009) Suppression of cell growth and invasion by miR-205 in breast cancer. *Cell Res.*, **19**, 439–448.
49. Gregory, P.A., Bert, A.G., Paterson, E.L., Barry, S.C., Tsykin, A., Farshid, G., Vadas, M.A., Khew-Goodall, Y. and Goodall, G.J. (2008) The miR-200 family and miR-205 regulate epithelial to mesenchymal transition by targeting ZEB1 and SIP1. *Nat. Cell Biol.*, **10**, 593–601.
50. Kent, O.A., Fox-Talbot, K. and Halushka, M.K. (2013) RREB1 repressed miR-143/145 modulates KRAS signaling through downregulation of multiple targets. *Oncogene*, **32**, 2576–2585.
51. Sempere, L.F., Freemantle, S., Pitha-Rowe, I., Moss, E., Dmitrovsky, E. and Ambros, V. (2004) Expression profiling of mammalian microRNAs uncovers a subset of brain-expressed microRNAs with possible roles in murine and human neuronal differentiation. *Genome Biol.*, **5**, R13.
52. Bartel, D.P. (2009) MicroRNAs: target recognition and regulatory functions. *Cell*, **136**, 215–233.
53. Shin, C., Nam, J.W., Farh, K.K., Chiang, H.R., Shkumatava, A. and Bartel, D.P. (2010) Expanding the microRNA targeting code: functional sites with centered pairing. *Mol. Cell*, **38**, 789–802.
54. Helwak, A., Kudla, G., Dudnakova, T. and Tollervey, D. (2013) Mapping the human miRNA interactome by CLASH reveals frequent noncanonical binding. *Cell*, **153**, 654–665.
55. Chi, S.W., Zang, J.B., Mele, A. and Darnell, R.B. (2009) Argonaute HITS-CLIP decodes microRNA-mRNA interaction maps. *Nature*, **460**, 479–486.
56. Hafner, M., Landthaler, M., Burger, L., Khorshid, M., Hausser, J., Berninger, P., Rothballer, A., Ascano, M. Jr, Jungkamp, A.C., Munschauer, M. *et al.* (2010) Transcriptome-wide identification of RNA-binding protein and microRNA target sites by PAR-CLIP. *Cell*, **141**, 129–141.
57. Kozomara, A. and Griffiths-Jones, S. (2011) miRBase: integrating microRNA annotation and deep-sequencing data. *Nucleic Acids Res.*, **39**, D152–D157.
58. Meyer, L.R., Zweig, A.S., Hinrichs, A.S., Karolchik, D., Kuhn, R.M., Wong, M., Sloan, C.A., Rosenbloom, K.R., Roe, G., Rhead, B. *et al.* (2013) The UCSC Genome Browser database: extensions and updates 2013. *Nucleic Acids Res.*, **41**, D64–D69.
59. Grimson, A., Farh, K.K., Johnston, W.K., Garrett-Engele, P., Lim, L.P. and Bartel, D.P. (2007) MicroRNA targeting specificity in mammals: determinants beyond seed pairing. *Mol. Cell*, **27**, 91–105.
60. Matys, V., Fricke, E., Geffers, R., Gossling, E., Haubrock, M., Hehl, R., Hornischer, K., Karas, D., Kel, A.E., Kel-Margoulis, O.V. *et al.* (2003) TRANSFAC: transcriptional regulation, from patterns to profiles. *Nucleic Acids Res.*, **31**, 374–378.
61. Flicek, P., Amode, M.R., Barrell, D., Beal, K., Brent, S., Carvalho-Silva, D., Clapham, P., Coates, G., Fairley, S., Fitzgerald, S. *et al.* (2012) Ensembl 2012. *Nucleic Acids Res.*, **40**, D84–D90.
62. Fineberg, S.K., Datta, P., Stein, C.S. and Davidson, B.L. (2012) MiR-34a represses Numbl in murine neural progenitor cells and antagonizes neuronal differentiation. *PLoS One*, **7**, e38562.